ADVANCED OPTICAL MATERIALS
www.advopticalmat.de

Scalable Noninvasive Organic Fiber Lithography for Large-Area Optoelectronics

*Himchan Cho, Su-Hun Jeong, Sung-Yong Min, Tae-Hee Han, Min-Ho Park, Young-Hoon Kim, Wentao Xu, and Tae-Woo Lee**

The development of precise, chemical-free, and low-cost pixel patterning with high resolution and throughput instead of conventional photolithography is very important for large-area flexible organic light-emitting diode (OLED) displays or solid-state lightings with high aperture ratio. Here, a novel scalable and noninvasive lithography is reported as a pixel patterning method for OLEDs using highly aligned printed organic fiber arrays in large area. Use of electrohydrodynamic organic nanowire printing (ONP) enables high-speed large-area fabrication and precise positioning of poly(9-vinylcarbazole) (PVK) fiber pixel separator arrays without chemical damage. Due to circular cross-section of PVK fibers, clear and effective separation of organic and metal cathode layers by PVK fibers is achieved. Easy control of interfiber separation in ONP also enables the demonstration of green OLED subpixels with different pixel widths (400, 200, 100 μm), which shows almost the same current efficiency and luminance as OLEDs without PVK fibers; i.e., PVK fiber pixel separators in OLEDs do not degrade OLED characteristics because the devices maintain almost the same electroluminescent area. Furthermore, it is demonstrated that individually well-aligned organic fibers are useful for pixel patterning of large-area, flexible OLEDs by fabricating a large-area (3 cm × 3 cm) white OLED and a flexible dot–matrix-display-type OLED.

1. Introduction

Recent advances in organic large-area electronics and optoelectronics are mainly based on the development of large-area patterning methods.[1] Simple, accurate, and quick patterning of unit devices and the related parts in large-area is very important to achieve low-cost mass production of products with high reliability and throughput. The conventional method for organic materials is vacuum deposition using metal shadow masks prepatterned in several hundred micrometer scale, but this method is not suitable for fabrication of highly integrated large-area devices due to its limited resolution and low throughput.[2,3]

H. Cho, S.-H. Jeong, Dr. S.-Y. Min, Dr. T.-H. Han, M.-H. Park, Y.-H. Kim, Dr. W. Xu, Prof. T.-W. Lee
Department of Materials Science and Engineering
Pohang University of Science and Technology (POSTECH)
77 Cheongam-Ro, Nam-Gu, Pohang, Gyeongbuk 37673, Republic of Korea
E-mail: twlee@postech.ac.kr, taewlees@gmail.com

DOI: 10.1002/adom.201600005

In organic light-emitting diodes (OLEDs), precise and low-cost pixel patterning is especially important for high-resolution large-area flexible displays. OLED pixels are defined by forming matrix patterns of anode and cathode, and the anode is usually patterned using photolithography. However, the choice of patterning process for organic layers and cathode is limited because the process should not damage the underlying organic layers.[3–5] One typical method for pixel separation is to use negatively tapered insulating photoresist patterns that are formed on a prepatterned indium tin oxide (ITO) substrate by photolithography.[3,4,6] However, the separator-formation process, photolithography, has disadvantages in fabrication of large-area flexible displays, because it is time-consuming, complex, and expensive due to several chemical steps, has low throughput, and may deteriorate the surface electronic structures of ITO due to the chemical process and organic residues.[7,8] Also, forming precise patterns on a nonplanar substrate by photolithography has been a major challenge.[7,9] Furthermore, limited pattern resolution is caused by diffraction of light and limited depth of field.[7,9] Several other pixel-patterning methods include microcontact printing,[10] imprint lithography,[11] soft-contact lamination,[12] micromolding in capillaries,[13] cold welding,[14] cathode transfer,[5] laser ablation,[15] spin-on patterning,[2] and detachment patterning.[16] These methods can pattern pixels with their own advantages, but cannot simultaneously satisfy effective pixel separation, simplicity, low-cost, large-area process, high resolution, and prevention of damage to underlying organic layers. Therefore, to achieve efficient mass production of large-area flexible displays, a new pixel patterning process must be developed.

Here, we report a very simple, rapid, scalable, noninvasive, low-cost, and large-area lithography to fabricate patterned electronic devices even on nonplanar flexible substrates using printed organic fibers.

We used electro-hydrodynamic organic nanowire printing (ONP) to fabricate highly aligned organic fiber arrays to pattern OLEDs (**Figure 1**a). ONP is a high-speed printing process to print highly aligned organic or organic/inorganic hybrid nanowires.[17] ONP allows direct printing of organic micro- or nanowire arrays in parallel straight lines at desired positions

and orientations.[17–20] Organic fiber arrays fabricated using ONP can function as very effective pixel separators; that is, ONP can be a very effective process for OLED pixel patterning, and has many advantages. 1) ONP provides a straightforward and inexpensive process to fabricate pixel separators without the complex procedure and expensive equipment of invasive photolithography. 2) ONP allows a very high fiber printing speed, which much reduces OLED fabrication time. 3) Accurate control of pixel size and pixel-to-pixel distance is possible because ONP enables accurate control of interfiber separation and fiber diameter. 4) The large printing area of ONP makes it suitable for large-area OLED fabrication. 5) Precise separator patterns can be formed by ONP even on nonplanar substrates because the fiber printing process is not affected by diffraction of light, limitation in depth of field, or unwanted movement of substrates. 6) ONP does not damage underlying organic layers. 7) Due to high flexibility of polymer fibers, ONP can be used for pixel patterning of flexible OLEDs. 8) Organic fibers smaller than 1.8 μm are invisible to human eyes and the pattern area is extremely smaller than the area of the display and lighting panel devices so that they do not lose actual pixel area significantly unlike the previous pixel separators or banks, which leads to achievement of the same brightness in patterned OLED devices with that in unpatterned ones.

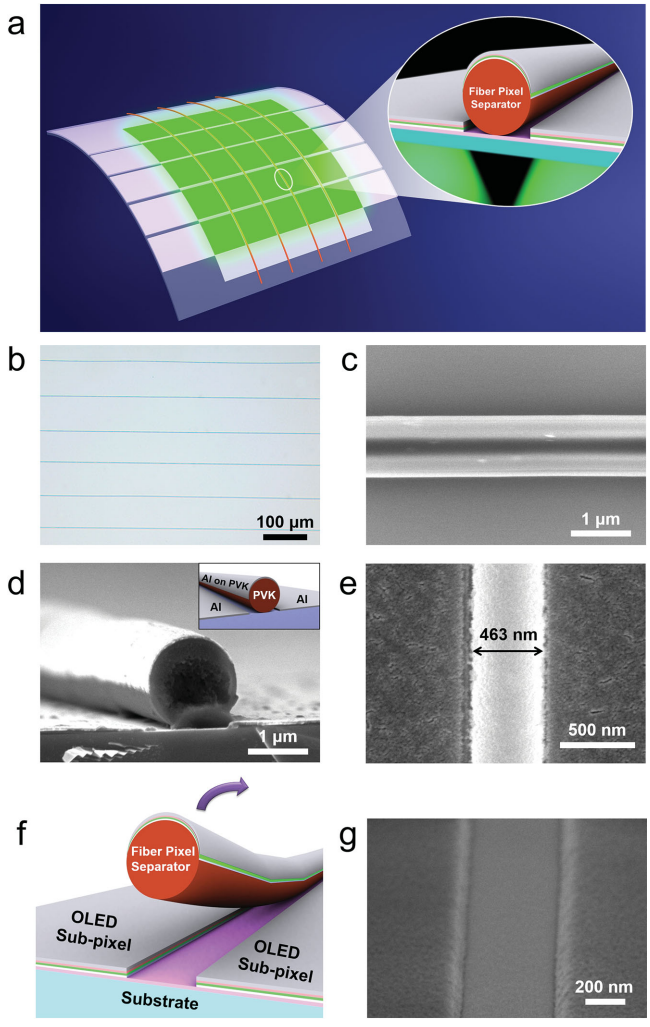

Figure 1. a) Schematic illustration showing the use of fiber pixel separators in OLEDs. b) Optical micrograph of a PVK fiber array with 70 μm interfiber separation. c) A SEM image of a PVK fiber with diameter of 1.01 μm. d) SEM image of PVK fibers on which 40 nm thick Al was deposited at cross-sectional view. Inset is a schematic illustration of the SEM image. e) SEM image of a PVK nanofiber on which 170 nm thick LiF was deposited. f) Schematic illustration showing the principle of organic fiber lithography. g) SEM image of separated LiF layer after removing the PVK nanofiber.

2. Results and Discussion

We used ONP to fabricate OLEDs that incorporate poly(9-vinylcarbazole) (PVK) fiber arrays as pixel separators with different interfiber separations, and confirmed that the PVK fibers can function effectively as pixel separators. OLEDs that incorporated 5, 10, 20, or 40 fiber pixel separators showed very similar characteristics to each other; this similarity demonstrates that the fiber pixel separators do not impede OLED characteristics. Furthermore, we demonstrated the potential of ONP for patterning large-area flexible OLEDs by fabricating a large-area (3 cm × 3 cm, 3 × 1 pixel) white OLED and a flexible dot-matrix-display-type OLED (3 cm × 3 cm, 5 × 5 pixels) in both of which the pixels were separated by PVK fiber arrays.

First, we developed an ONP process to print aligned PVK fibers with diameters from several hundreds of nanometers to ≈1 μm (Figure 1b–e, Figure S1, Supporting Information). PVK was chosen because of its nearly insulating property with very low hole mobility (4.8×10^{-9} cm^2 V^{-1} s^{-1}) without backbone conjugation,[21] high glass transition temperature (≈220 °C)[22] and ease of fiber printing originating from the high molecular weight (M_w = 1 100 000). Although PVK nanofibers with diameters of 400–500 nm were fine for pixel separation (Figure 1e), we used relatively thick fibers to increase the thickness of layers that can be separated by the fibers, and enhance insulation between pixels. Highly aligned PVK fiber arrays were fabricated using a highly concentrated solution of PVK/styrene (70 mg mL^{-1}). The interfiber separation was almost constant at ≈70 μm (Figure 1b) and the average fiber diameter was 1.11 ± 0.12 μm (Figure 1c). Before the PVK fiber arrays were introduced to OLEDs, we tested whether the fibers can work well as pixel separators by depositing 40 nm Al on the fiber arrays without sample rotation during thermal evaporation. We confirmed that the fibers can separate the Al layer very effectively (Figure 1d, Figure S1a, Figure S2, Supporting Information). The edges of separated Al layers were clearly visible in cross-sectional (Figure 1d) and 45° tilted views (Figure S1a, Supporting Information). The effective separation is mainly due to the circular cross-sectional shape of PVK fibers (Figure 1d). After vacuum deposition process, the fiber pixel separators can be detached by the taping method as previously reported when it is necessary (Figure 1f,g).[17]

We then fabricated OLEDs that incorporated PVK fiber arrays as pixel separators (**Figure 2**); the detailed process is explained in the experimental section. We fabricated the PVK fiber arrays on spin-coated hole injection layers (HIL). Because we can use ONP to control the positions of the fiber arrays accurately, they can be located exactly in the pixels. Also, the widths and the

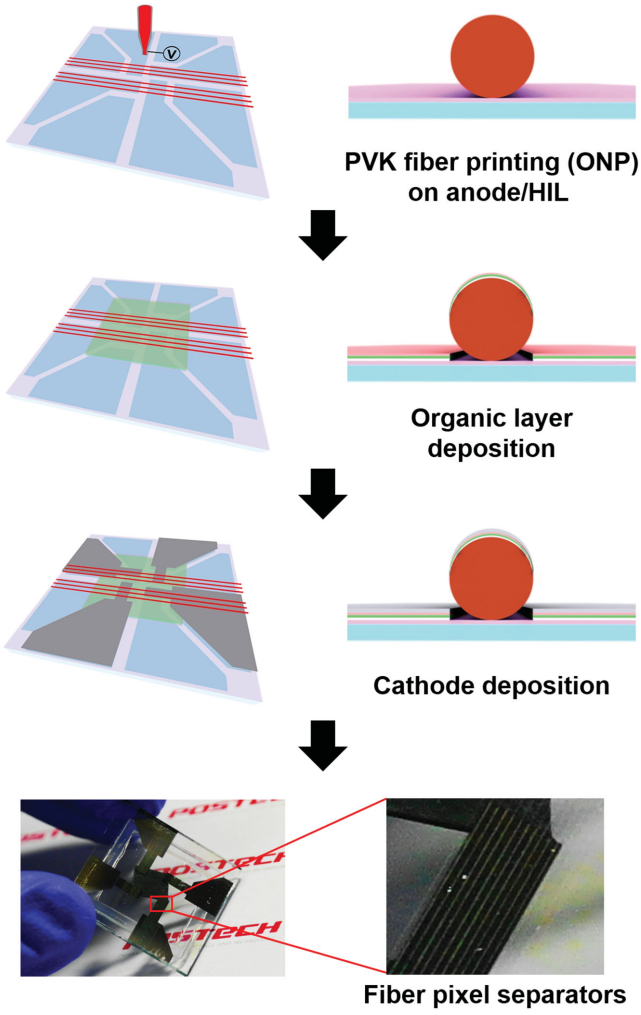

Figure 2. Schematic diagrams describing OLED fabrication procedure incorporating fiber pixel separator arrays. The photographs show the fiber pixel separator array in a pixel.

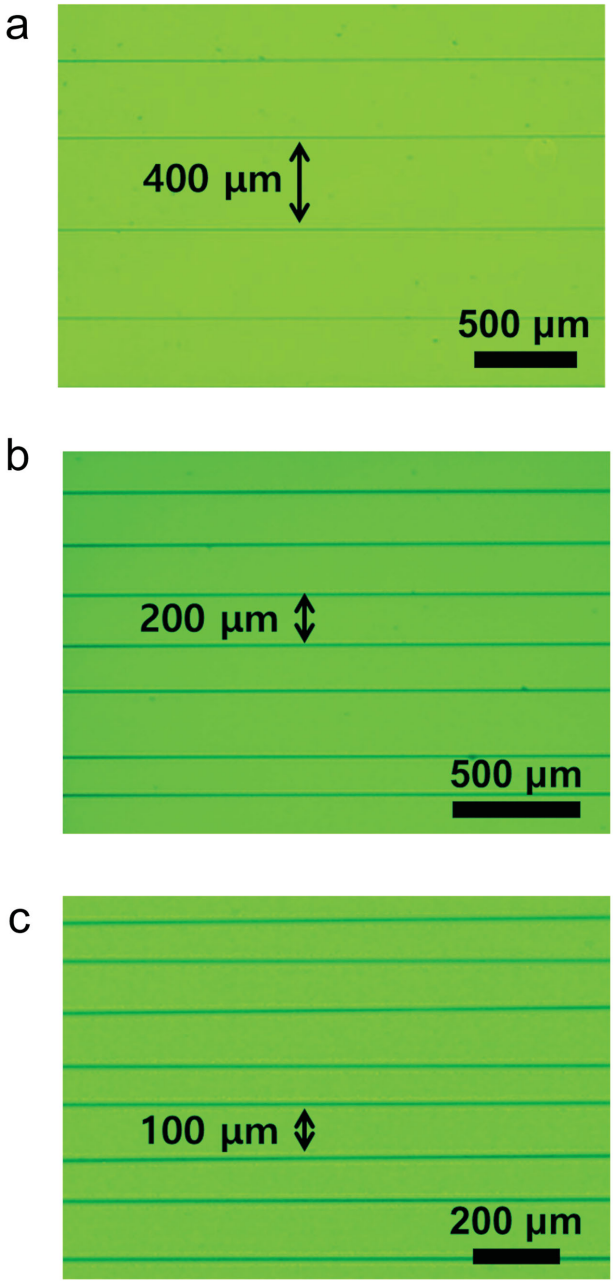

Figure 3. Stereoscopic micrographs of the green OLED pixels incorporating fiber pixel separator arrays of a) 400 μm, b) 200 μm, and c) 100 μm interfiber separation during light emission.

numbers of subpixels can be freely controlled by adjusting interfiber separation. We fabricated green OLED pixels that have fiber pixel separators with varying interfiber separation (400, 200, and 100 μm), and captured stereoscopic micrographs during light emission (**Figure 3**). To connect all subpixels and to turn them on at the same time for visualization, the edges of fiber pixel separators were cut before deposition of organic layers and cathode. To confirm the formation of subpixels by fiber pixel separators, two horizontal and one vertical PVK fiber were printed on a pixel (**Figure 4**); the edges of horizontal fibers were cut before deposition. The absence of light emission by the portion of the pixel to the right of the vertical fiber demonstrates effective pixel separation.

To determine whether incorporation of PVK fibers affected OLED characteristics, we compared the characteristics of OLEDs incorporating 0, 5, 10, 20, and 40 PVK fiber pixel separators (**Figure 5**). The maximum current efficiencies (96.5 cd A^{-1}) of the OLEDs with PVK fiber pixel separators were similar to those of the OLED without them (93.4, 95.8, 91.5 and 94.4 cd A^{-1} for OLEDs with 5, 10, 20, and 40 fibers, respectively) (Figure 5a); the deviations were within a range of ≈5%: The devices using 40 fibers (94.4 cd A^{-1}) showed almost the same efficiency with that without any pixel separating fibers (96.5 cd A^{-1}), which demonstrates that our patterning fibers do not contribute to loss of the pixel area. Furthermore, the OLEDs showed almost the same luminance (Figure 5b) and current density (Figure 5c); these results demonstrate that incorporation of PVK fibers does not degrade OLED characteristics.

The use of fiber pixel separators can be easily applied to various types of OLEDs. We also fabricated white OLEDs that have fiber pixel separators with 200 μm interfiber separation (**Figure 6**). To

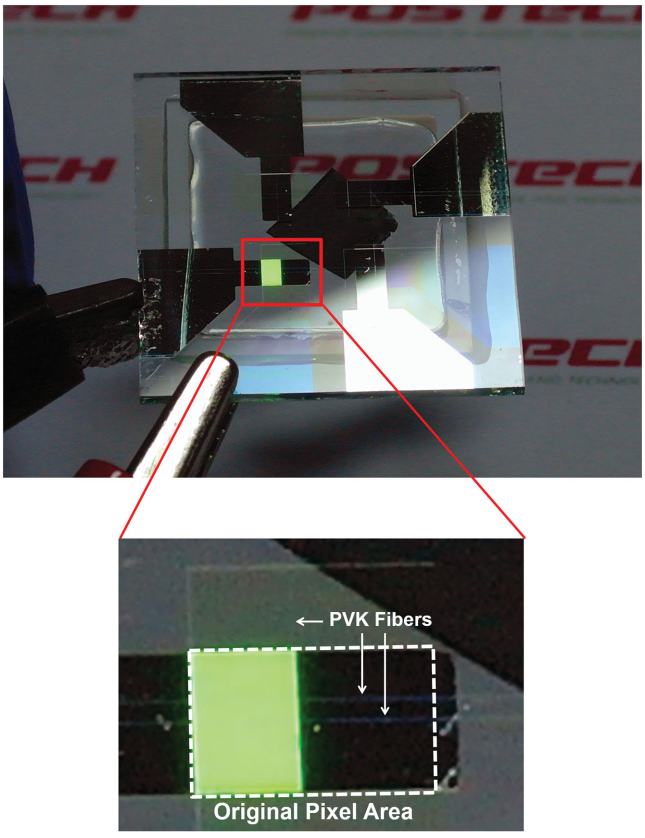

Figure 4. Photograph of green OLED pixel incorporating two horizontal and one vertical PVK fiber pixel separators.

show that fiber pixel separators can be patterned in large scale, we fabricated a 3 cm × 3 cm large-area white OLED (**Figure 7**a). The 3 cm × 3 cm original pixel was clearly divided into three 3 cm × 1 cm subpixels by two parallel PVK fiber pixel separators. The patterning area can be further increased by increasing the size of the printer collector. In addition, to demonstrate that the fiber pixel separators can be used practically for simple passive-matrix OLED displays, we fabricated a large-area (3 cm × 3 cm) flexible dot-matrix-display-type OLED with 5 × 5 pixels (Figure 7b). To show pixel separation at one time, only 1, 3, 5 rows and columns of subpixels were electrically contacted. This result also demonstrates that PVK fiber pixel separators can be patterned, and work well on flexible substrates. Due to flexibility of PVK fibers, the pixel separation remained stable during bending. These demonstrations show the potential of fiber pixel separators for use in OLED lighting and display products. We envision that the fiber pixel patterning can be eventually employed in commercial RGB-patterned OLEDs as shown in the schematic diagram (Figure S3, Supporting Information).

3. Conclusion

In conclusion, we have reported a rapid, scalable, and noninvasive lithography that uses highly aligned organic fiber arrays for pixel patterning in OLEDs. We optimized ONP process to

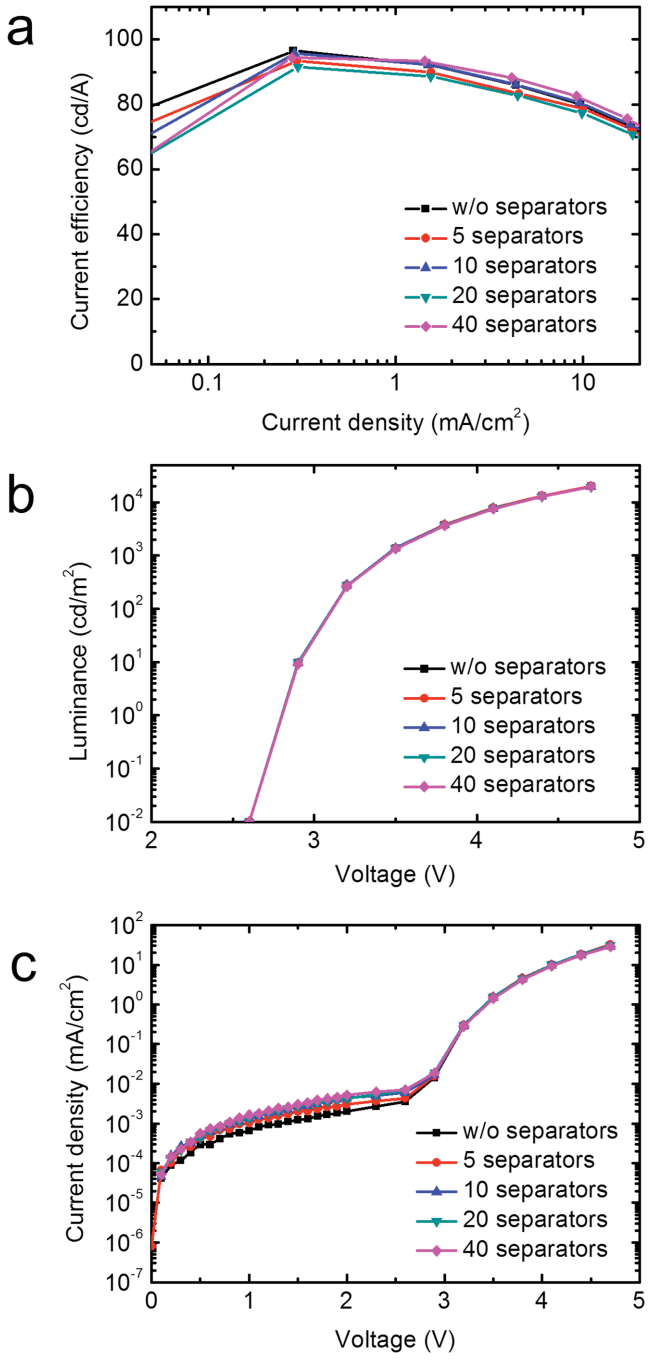

Figure 5. a) Current efficiency, b) luminance, and c) current density of green OLEDs incorporating 5, 10, 20 and 40 PVK fiber pixel separator arrays (400, 200, 100, and 50 μm interfiber separation, respectively).

fabricate PVK micro- or nanofiber arrays with various diameters and confirmed that they can be used as pixel separators in OLEDs. Due to circular cross-section of PVK fibers, clear and effective separation of organic and metal cathode layers by PVK fibers was achieved. Easy control of interfiber separation in ONP enabled the demonstration of green OLED subpixels with different pixel widths (400, 200, 100 μm). OLEDs with 5, 10, 20, or 40 PVK fiber pixel separators showed almost the

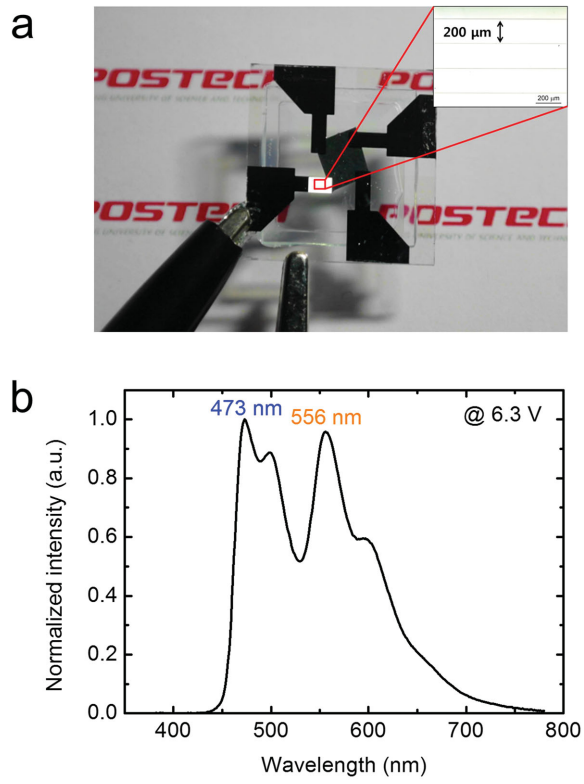

Figure 6. a) Photograph of the white OLED incorporating a PVK fiber pixel separator array of 200 μm interfiber separation. Inset: Optical micrograph of the white-emitting pixel. b) Electroluminescence spectrum of the white OLED.

same current efficiency and luminance with those of OLEDs without them; i.e., PVK fiber pixel separators in OLEDs do not degrade OLED characteristics because the devices maintain almost the same electroluminescent area. Furthermore, we demonstrated that individually well-aligned organic fibers are useful for pixel patterning of large-area, flexible OLEDs by fabricating large-area (3 cm × 3 cm) white OLED and flexible dot-matrix-display-type OLED.

ONP-based patterning has many advantages as a new patterning process for OLEDs, including simplicity, low-cost, high process speed, high throughput, noninvasiveness, easy and accurate control of separator position and pitch, and the possibility of patterning large-area, flexible OLEDs. Therefore, this process can provide a simple and effective method to pattern the pixels in flat or flexible OLEDs. Furthermore, we expect that our method can be also applied to patterning of column spacers or banks in active matrix OLEDs and of grid patterns in large-area white OLEDs. We believe that our work presents an innovative way to increase brightness in the same area (or aperture ratio) and resolution of panel devices in the display and lighting industries.

4. Experimental Section

Fabrication of PVK Fiber Arrays Using ONP: PVK (M_w = 1 100 000) and styrene were purchased from Sigma-Aldrich. To obtain ≈1 μm scale PVK fibers, PVK in styrene solution (68.5 mg mL^{-1}) was injected through the metal nozzle at a feed rate of 120 nL min^{-1}. Tip-to-collector distance was 4.0 mm and 2.2–2.4 kV of D.C. voltage was applied to the nozzle. While the collector was moving, highly aligned PVK fibers were printed on the substrates or devices. For the PVK nanofibers with smaller scale in Figure 1e and Figure S1b-e (Supporting Information), PVK/styrene solution of 56.2 mg mL^{-1} was used at a feed rate of 200 nL min^{-1}. For the thicker PVK nanofibers (Figure S1f,g, Supporting Information), PVK/styrene solution of 59.1 mg mL^{-1} was used at a feed rate of 150 nL min^{-1} and tip-to-collector distance of 5.5 mm.

OLED Fabrication: Prepatterned ITO anodes (pixel area: 2 mm × 3 mm) on glass substrates were sonicated with acetone and isopropyl alcohol in the ultrasonic bath and boiled on a hot plate to evaporate solvent immediately. After UV/O_3-treatment for 15 min, a mixture of poly(3,4-ethylenedioxythiophene):poly(styrenesulfonate) (PEDOT:PSS) (Clevios

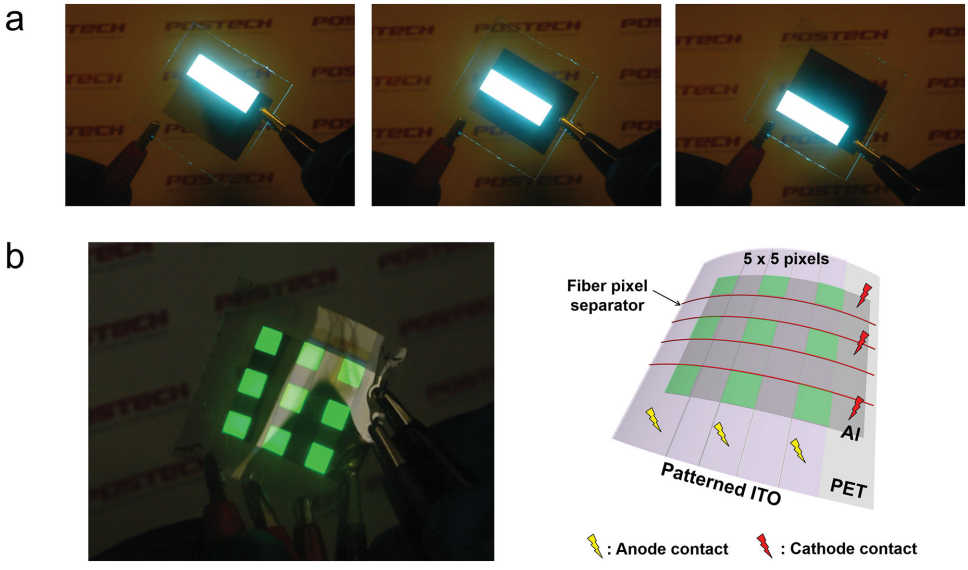

Figure 7. a) The photographs of 3 cm × 3 cm large-area white OLED patterned into three 3 cm × 1 cm subpixels by PVK fiber pixel separators. b) The photograph (left) and schematic diagram (right) of a flexible dot-matrix-type OLED display with 25 pixels patterned by PVK fiber pixel separators.

P VP AI4083) and a perfluorinated polymeric acid, tetrafluoroethylene-perfluoro-3,6-dioxa-4-methyl-7-octene-sulfonic acid copolymer (PFI) (Sigma-Aldrich) was spin-coated to fabricate a HIL of 50 nm thickness (PEDOT:PSS:PFI = 1:6:12.7 (w:w:w)), then baked at 150 °C for 30 min in air. The ONP was used to print highly-aligned PVK fibers on the HIL. After ONP, the specimens were transferred to a high-vacuum thermal evaporator (<10^{-7} Torr), and a 15 nm thick hole transporting layer of di-[4-(*N*,*N*-ditolyl-amino)-phenyl]cyclohexane (TAPC) was deposited on the HIL.

To fabricate phosphorescent green OLEDs, a green-emitting dopant material, bis(2-phenylpyridine) (acetylacetonate) iridium(III) ($Ir(ppy)_2(acac)$) was doped into two different host layers (5 nm for both layers) of 4,4′,4″-tris(carbazol-9-yl)triphenylamine (TCTA) and 4,4′-bis(carbazol-9-yl)biphenyl (CBP). The host:dopant ratios of TCTA:$Ir(ppy)_2(acac)$ and CBP:$Ir(ppy)_2(acac)$ were 100:3 and 100:4, respectively. 2,2′,2″-(1,3,5-benzinetriyl)-tris(1-phenyl-1-H-benzimidazole) (TPBI) (55 nm) was used as an electron transporting layer (ETL). Then, LiF (1 nm) and Al (40 nm) were deposited in sequence. The device structure was ITO (185 nm)/HIL (50 nm)/TAPC (15 nm)/TCTA:$Ir(ppy)_2(acac)$ (5 nm)/CBP:$Ir(ppy)_2(acac)$ (5 nm)/TPBI (55 nm)/LiF (1 nm)/Al (40 nm).

For phosphorescent white OLEDs, a blue-emitting dopant material, bis(3,5-difluoro-2-(2-pyridyl)phenyl-(2-carboxypyridyl)iridium(III) (FIrpic) was doped into two different host layers (6.7 nm for both layers) of TCTA and 2,6-bis(3-(9H-carbazol-9-yl)phenyl)pyridine (DCzppy). The host:dopant ratios of TCTA:FIrpic and DCzppy:FIrpic were 100:7 and 100:20. The orange-emitting dopant material, bis(2-phenylbenzothiazolato)(acetylacetonate)iridium(III) ($Bt_2Ir(acac)$) was doped into a host layer of DCzppy (0.6 nm). The host:dopant ratio of DCzppy:$Bt_2Ir(acac)$ was 100:3. Tris(2,4,6-trimethyl-3-(pyridin-3-yl)phenyl) borane (3TPYMB) (40 nm) was used as an ETL. Then, LiF (1 nm) and Al (40 nm) were deposited in sequence. The device structure was ITO (185 nm)/HIL (50 nm)/TAPC (15 nm)/TCTA:FIrpic (6.7 nm)/DCzppy:$Bt_2Ir(acac)$ (0.6 nm)/DCzppy:FIrpic (6.7 nm)/3TPYMB (40 nm)/LiF (1 nm)/Al (40 nm). All OLEDs were encapsulated using UV curable epoxy resin in inert atmosphere.

Supporting Information

Supporting Information is available from the Wiley Online Library or from the author.

Acknowledgements

This work was supported by the research funds from an IITP ICT Consilience Creative Program (IITP-2015-R0346-15-1007) of the Ministry of Science, ICT and Future Planning. This work was also supported by the Center for Advanced Soft-Electronics funded by the Ministry of Science, ICT and Future Planning as Global Frontier Project (2014M3A6A5060947).

Received: January 4, 2016
Revised: February 5, 2016
Published online: March 9, 2016

[1] a) E. Menard, M. A. Meitl, Y. Sun, J.-U. Park, D. J.-L. Shir, Y.-S. Nam, S. Jeon, J. A. Rogers, *Chem. Rev.* **2007**, *107*, 1117; b) A. L. Briseno, S. C. B. Mannsfeld, M. M. Ling, S. Liu, R. J. Tseng, C. Reese, M. E. Robertz, Y. Yang, F. Wudl, Z. Bao, *Nature* **2006**, *444*, 913; c) G. J. McGraw, S. R. Forrest, *Adv. Mater.* **2013**, *25*, 1583; d) S.-J. Jeong, G. Xia, B. H. Kim, D. O. Shin, S.-H. Kwon, S.-W. Kang, S. O. Kim, *Adv. Mater.* **2008**, *20*, 1898.
[2] J. Jeong, D. Mascaro, S. Blair, *Org. Electron.* **2011**, *12*, 2095.
[3] Z. H. Huang, G. J. Qi, X. T. Zeng, W. M. Su, *Thin Solid Films* **2006**, *503*, 246.
[4] K. Nagayama, T. Yahagi, H. Nakada, T. Tohma, T. Watanabe, K. Yoshida, S. Miyaguchi, *Jpn. J. Appl. Phys.* **1997**, *36*, L1555.
[5] J. Rhee, H. H. Lee, *Appl. Phys. Lett.* **2002**, *81*, 4165.
[6] J. Rhee, J. Park, S. Kwon, H. Yoon, H. H. Lee, *Adv. Mater.* **2003**, *15*, 1075.
[7] Y. Xia, G. M. Whitesides, *Annu. Rev. Mater. Sci.* **1998**, *28*, 153.
[8] M. Henry, J. Wendland, P. M. Harrison, D. Hand, *presented at 26th ICALEO*, Crawley, Sussex, England (November 2007).
[9] a) R. J. Jackman, J. L. Wilbur, G. M. Whitesides, *Science* **1995**, *269*, 664; b) S. Seraji, Y. Wu, N. E. Jewell-Larson, M. J. Forbess, S. J. Limmer, T. P. Chou, G. Cao, *Adv. Mater.* **2000**, *12*, 1421; c) W. D. Deininger, C. E. Garner, *J. Vac. Sci. Technol. B* **1988**, *6*, 337.
[10] a) A. Kumar, G. M. Whitesides, *Appl. Phys. Lett.* **1993**, *63*, 2002; b) J. A. Rogers, Z. Bao, K. Baldwin, A. Dodabalapur, B. Crone, V. R. Raju, V. Kuck, H. Katz, K. Amundson, J. Ewing, P. Drzaic, *Proc. Natl. Acad. Sci.* **2001**, *98*, 4835.
[11] L. J. Guo, *Adv. Mater.* **2007**, *19*, 495.
[12] a) T.-W. Lee, J. Zaumseil, Z. Bao, J. W. P. Hsu, J. A. Rogers, *Proc. Natl. Acad. Sci.* **2004**, *101*, 429; b) T.-W. Lee, J. Zaumseil, S. H. Kim, J. W. P. Hsu, *Adv. Mater.* **2004**, *16*, 2040; c) Y.-L. Loo, T. Someya, K. W. Baldwin, Z. Bao, P. Ho, A. Dodabalapur, H. E. Katz, J. A. Rogers, *Proc. Natl. Acad. Sci.* **2002**, *99*, 10252; d) T.-W. Lee, S. Jeon, J. Maria, J. Zaumseil, J. W. P. Hsu, J. A. Rogers, *Adv. Funct. Mater.* **2005**. *15*: 1435.
[13] W. S. Beh, I. T. Kim, D. Qin, Y. Xia, G. M. Whitesides, *Adv. Mater.* **1999**, *11*, 1038.
[14] C. Kim, P. E. Burrows, S. R. Forrest, *Science* **2000**, *288*, 831.
[15] a) C. Liu, G. Zhu, D. Liu, *Displays* **2008**, *29*, 536; b) R. Mandamparambil, H. Fledderus, G. V. Steenberge, A. Dietzel, *Opt. Express* **2010**, *18*, 7575.
[16] J.-H. Choi, D. Kim, P. J. Yoo, H. H. Lee, *Adv. Mater.* **2005**, *17*, 166.
[17] S.-Y. Min, T.-S. Kim, B. J. Kim, H. Cho, Y.-Y. Noh, H. Yang, J. H. Cho, T.-W. Lee, *Nat. Commun.* **2013**, *4*, 1773.
[18] Y. Lee, T. S. Kim, S.-Y. Min, W. Xu, S.-H. Jeong, H.-K. Seo, T.-W. Lee, *Adv. Mater.* **2014**, *26*, 8010.
[19] S. Hwang, S.-Y. Min, I. Bae, S. Cho, K. Kim, T.-W. Lee, C. Park, *Small* **2014**, *10*, 1976.
[20] a) W. Xu, H.-K. Seo, S.-Y. Min, H. Cho, T.-S. Lim, C.-Y. Oh, Y. Lee, T.-W. Lee, *Adv. Mater.* **2014**, *26*, 3459; b) W. Xu, T.-S. Lim, H.-K. Seo, S.-Y. Min, H. Cho, M.-H. Park, Y.-H. Kim, T.-W. Lee, *Small* **2014**, *10*, 1999; c) W. Xu, L. Wang, Y. Liu, S. Thomas, H.-K. Seo, K.-I. Kim, K. S. Kim, T.-W. Lee, *Adv. Mater.* **2015**, *27*, 1619.
[21] P. D'Angelo, M. Barra, A. Cassinese, M. G. Maglione, P. Vacca, C. Minarini, A. Rubino, *Solid-State Electron.* **2007**, *51*, 123.
[22] M.-A. Tehfe, S. Elkoun, M. Robert, *Appl. Sci.* **2015**, *5*, 241.